Research on Engineering Structures & Materials
www.jresm.org
Research Group

Research Article

Experimental investigation on the bond behavior of the GFRP bars with one-part geopolymer concrete and conventional concrete

Guruprasad T N [*,1,2,a], M H Prashanth [1,b], Mahanthesh H S [2,c], Narasimhan M.C [1,d]

[1]*Dept. of Civil Eng., National Institute of Technology Karnataka, Mangalore, Karnataka, India*
[2]*Dept. of Civil Eng., Sri Siddhartha Institute of Technology, Tumakuru, Karnataka, India*

Article Info

Article History:

Received 22 Jan 2026

Accepted 20 Apr 2026

Keywords:

GFRP bars;
One-part geopolymer Concrete;
Bond strength;
Bond stress;
Versus slip relation;
Pullout test

Abstract

The current study investigates the binding behavior of steel bars and GFRP in ordinary Portland cement concrete (OPCC) and one-part geopolymer concrete (OPGC). The maximum pullout load as well as features at failure were examined in relation to the kind of concrete, bar diameter, and bar type. In one-part geopolymer concrete along with regular concrete, the pullout strengths and also adhesive properties of GFRP bond specimens were contrasted with steel bar specimens. An energy-based identical bond strength strategy was taken into consideration in order to suggest the bond durability at peak load. This showed that a bigger diameter results in a faster rate of strength decline, along with a decline in bond performance. Pullout load was observed in bond specimens with smaller diameters, where bond strength regulated the shear strength within the GFRP bars along with ribs. In specimens of conventional concrete and one-part geopolymer concrete with diameters of 12 and 16 mm. There was evidence of concrete split failure, where the shear strength of the concrete determines the bond strength. The bond strength is positively impacted by rises in concrete's compressive strength, that spans from 14.57 to 32.12%.

1. Introduction

The building sector is vital to the economic success of any emerging nation, including India. However, its operations also have serious negative effects on the environment, which calls for a review of the sector's Environment Management Practices (EMPs). High energy consumption and an unchecked increase in greenhouse gas emissions are the results of increased cement manufacturing to support the nation's concrete infrastructure development [1]. The most common cementitious material is Portland cement, but producing one ton of Portland cement emits nearly one ton of CO_2[2], as well as the cement production process is responsible for between 5 and 8% of global CO_2 emissions. One of the main causes of global warming and its related effects on the ecosystem is the emission of greenhouse gases into the atmosphere, such as CO_2. As a result, creating a green cementitious substance that emits substantially less CO_2 during manufacture is essential [3]. Industrial by-products such as fly ash, ground granulated blast furnace slag (GGBS), and silica fume are examples that have been incorporated to concrete for supplementary cementitious materials (SCMs) in recent decades in an effort to improve the material's qualities and lessen its carbon footprint [4]. However, because these materials must react with the cement hydration product to produce the binding property, they can only be utilized as partial substitutes of OPC. Therefore, there is a lot of interest in creating substitute binding materials which can preserve the necessary engineering qualities while

*Corresponding author: gurutn008@gmail.com
[a]orcid.org/0000-0001-7969-2756; [b]orcid.org/0000-0001-9435-3437; [c]orcid.org/0009-0008-5585-3744; [d]orcid.org/0000-0001-6094-1492
DOI: http://dx.doi.org/10.17515/resm2026-1474me0122rs

lowering the carbon footprint as well as embodied energy of final goods (like concrete). Alkali-activated binders (AABs) or even geopolymers are becoming a competitive alternative to OPC in the modern era because their mechanical and durability qualities are nearly equal to, and frequently better than, those of OPC-based mortars along with concretes, and they are less vulnerable to environmental effects [5]. Since AABs provide a way to value industrial by-products and do away with the need for OPCs, their increased use is also desirable. One practical strategy for creating environmentally friendly and sustainable building materials is to use these by-products, which are high in alumina-silicates (such as GGBFS, fly ash, etc.), as source material [6]. By using these resources in the production of concrete, it is possible to reduce the pollution of the air around it, soil, and water caused by industrial wastes as well as the negative environmental effects of increased cement production [7]. However, only about 25% and 65% of the FA and GGBFS generated worldwide, respectively, are thought to be used for other purposes at the moment[8].Traditional AABs, such as the so-called "geopolymers," are created as two-part mixes through the chemical reaction of a concentrated alkaline solvent with an aluminosilicate substrate (a precursors) material, which is typically taken as a sort of fine powder[9].The concentrated aqueous alkali silicates or otherwise hydroxides that make up the majority of the activator solutions [10] are generally corrosive and extremely viscous, making them difficult to utilize. Alkali activator solution preparation and use also call for extra care, strict safety precautions, and qualified personnel. As a result, the solution is frequently made 24 hours before it is mixed with a solid precursor. Mass production, broad commercialization, and the use of traditional two-part AABs are all greatly impacted by this. This problem, which involves managing the activator solutions, has motivated researchers to use solid activators to create one-part geopolymers (OPG) or one-part alkali-activated binder materials (OP-AAMs). One-part AAMs (OP-AAMs) have the distinct benefit of being simpler and safer to produce and use than their two-part counterparts, even if they are also shown to have functionally identical features to OPC-based materials. OP-AAMs are therefore a viable substitute for pre-cast and cast-in-situ applications in the building sector [1]. On the other hand, the most widely used building material for infrastructure development is steel-reinforced concrete. However, almost 7% of all CO2 emissions in the atmosphere, which cause global warming, are caused by the manufacture of cement [11]. Furthermore, it is projected that by 2060,6000 million of tons of Portland cement, or 1.5 times the amount produced now—will be consumed globally each year. With an 80% reduced carbon footprint than cement-based concrete, geopolymer concrete (GPC) can be used in its stead[12]. The durability of steel-reinforced concrete structures has also reduced significantly due to a number of deteriorating mechanisms, with reinforcement corrosion emerging as the most important and necessitating repair. Fiber-reinforced polymer (FRP) composite bars are a fantastic alternative to metal since they do not corrode, steel reinforcement in challenging conditions. Therefore, a more sustainable and long-lasting building material that is absent from traditional reinforced concrete structures would be supplied by fiber-reinforced polymer (FRP) bars reinforced in one-part geopolymer concrete. When researchers examined the bonding of GPC and OPCC to steel bars, they discovered that GPC has a stronger binding than OPCC if the two forms of concrete's compressive strengths were equal[13][14]. Additionally, it has been shown that the stress on the bond versus slip curve of the two concretes and failure pattern are identical[15].The binding behavior of GFRP bars using sea sand including seawater has been the subject of a few investigations [16], and [17]. After 28 days, [18] found that the binding strength of the GFRP bar using traditional and seawater concrete was little different, and reported that this difference was 15%. The specimens' binding strength decreased by 20% and 8%, respectively, following 250 days of exposure to seawater as well as its wet-dry cycles, and showed that the bond strength of the saltwater sea-sand concrete had dropped by 3% when comparing the bond endurance of GFRP reinforced conventional and seawater sea-sand concrete. Because there are no regulations for the surface treatment of FRP bars, unlike steel, there are numerous varieties of FRP bars available, such as sand-coated (SC), grooved, helically wrapped (HW), ribbed, among others. The bond strength of OPCC strengthened using SC as well as HW GFRP bars is the same, although being marginally lower than that of steel bars[19]. [20]discovered that the HW GFRP-reinforced OPCC performed better than the other surface

arrangements. Furthermore, they recommended strengthening concrete rather than changing the surface arrangement because the former has a greater impact on bond strength. The bond strength of OPCC using ribbed GFRP bars was higher than that of HW and HW-SC bars, according to[21].

Despite many advancements in the characterization of materials, research on the application of OPGC as a structural member remains limited. In contrast, conventional concrete with steel has been extensively studied. The scarcity of OPGC experimental data with respect to the response of load deformation, particularly when reinforced with GFRP bars as an alternative material, highlights a crucial research gap for the study. Also, the literature research indicates that there is a significant knowledge gap on how various FRP bar types, surface designs, and compressive strength of concrete affect the bonding performance using geopolymer concrete (GPC) supplemented with FRP bars. Few studies have been conducted on the bonding properties of GFRP bars in GPC, yet none have specifically looked at how well they work in one-part geopolymer concrete (OPGC). The current study experimentally investigates the bond behavior of GFRP bars implanted in conventional concrete with one-part GPC in order to close this gap. Additionally, a comparison of steel and GFRP bars is carried out, paying close attention to the impacts of concrete strength, bar type, and bar diameter.

2. Program for Experimentation

2.1 Materials

2.1.1 Design of a Concrete Mix

The current study used sustainable industrial waste materials, such as fly ash of class F coming from thermal power stations as well as ground granulated blast furnace slag (GGBS) leftover from steel production, as precursors to create one-part geopolymer concrete. The chemical makeup of fly ash as well as GGBS is presented in Table 1. Their relative specific gravities are 2.15 and 2.75. Powdered anhydrous sodium metasilicate is utilized as an activator. Gravel is used as coarse aggregate (CA) and M sand as fine aggregate (FA) in this study. The physical attributes of the FA and CA that were obtained in accordance with IS 2386-1967, part 3, are listed in Table 2. Three sets of specimens were taken into consideration for each test, and the average results are listed in Table 2. The IS-383-2016 code was followed in the sieve analysis of FA and CA. FA was discovered to be a member of Zone II. Both aggregates meet IS 383-1970's codal requirements. Table 3 displays both the normal concrete of grade M40 and the ideal mix portion of one-part geopolymer concrete with the same grade. Three 150mm cubes were cast and tested for compressive strength. Normal concrete cubes were kept in water for curing for 28 days, and OPGC cubes were cured under ambient conditions. The average values of the normal M40 grade concrete and optimum one-part geopolymer concrete were 44.71MPa and 54.36 MPa, respectively, and the calculated standard deviation is tabulated in Table 4.

Table 1. XRF analysis of the chemical makeup of FA and GGBS in % weight

Material	Al_2O_3	BaO	CaO	Cr_2O_3	Fe_2O_3	K_2O	MgO	MnO	Na_2O	P_2O_5	SO_3	SiO_2	TiO_2
FA	25.31	0.07	12.25	0.01	9.9	0.64	1.14	0.14	0.32	0.51	0.57	46.04	1.46
GGBS	13.8	0.06	42.13	0	0.58	0.32	5.76	0.27	0.2	0.034	3.33	32.92	0.57

Table 2. The physical characteristics of F.A. and C.A.

Sample	Specific gravity	Absorption of water (%)	Fineness modulus (%)
Coarse aggregate	2.73	0.83	4.42
Fine aggregate	2.56	2.44	3.78

Table 3. Mix proportion of M40 grade and one-part geopolymer concrete

Type of concrete	Cement (kg m^{-3})	Fly ash (kg m^{-3})	GGBS (kg m^{-3})	C.A (kg m^{-3})	F.A (kg m^{-3})	Water (kg m^{-3})	Activator (kg m^{-3})	Superplasticizer (kg m^{-3})
M40 grade of concrete (OPCC)	440	.....	....	918	754	176	.....	
One-part geopolymer concrete (OPGC)	.....	190.8	224.19	925.15	697.41	180	56.25	3.6

Table 4. Compressive strength outcomes

Concrete type	Compressive strength (MPa)				SD
	Sample1	Sample2	Sample3	Mean	
M40 grade of concrete (OPCC)	45.33	46	42.8	44.71	1.68
One-part geopolymer concrete (OPGC)	58.66	48.88	55.55	54.36	4.99

2.1.2 Properties of Rebar

GFRP along with Fe415 HYSD bars of steel had been used in this investigation as cement concrete reinforcement. GFRP bars are composed of 15% to 25% resin and 75% to 85% glass fiber by weight[16]. Table 5 lists the mechanical characteristics of steel and GFRP bars. In accordance with ASTM rules, the manufacturer conducted a tension test upon GFRP bars.

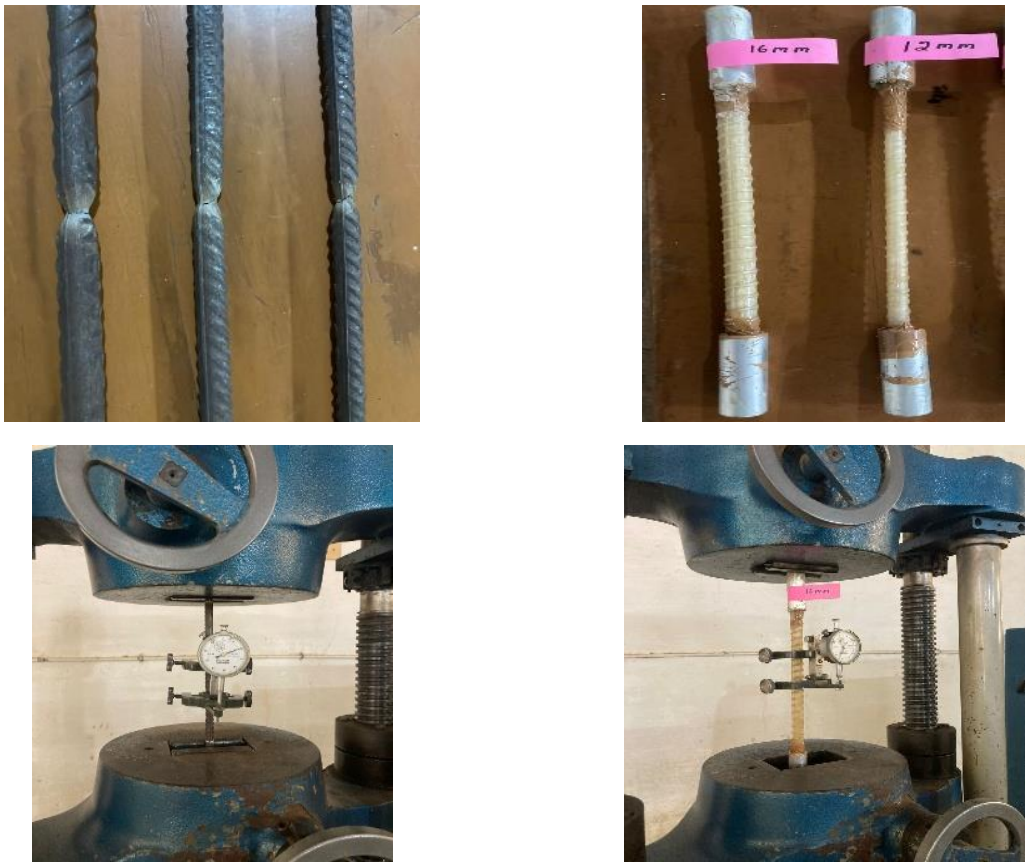

Fig. 1. Test setup for steel bars and GFRP bars

400mm length of samples were obtained in order to perform mechanical testing and evaluate the specimen's ultimate elongation, elastic modulus, and tensile strength; table 5 shows the typical outcome. The test arrangement used in the lab is depicted in Figure 1. In our lab, the tension test on steel bars was performed utilizing 600mm-long samples in accordance with IS:

1786-20008 codal requirement. Additionally, Table 5 tabulates the computed yield strength, ultimate strength, and elastic modulus average values.

Table 5 Steel's and GFRP bars' mechanical characteristics

Types	Bar's nominal diameter(mm)	Measured diameter of bar (mm)	Yield strength (MPa)	Ultimate tensile strength (MPa)	Elastic modulus (MPa)	Ultimate percentage of elongations
GFRP	10	9.94	-	978.56	51.76	3.31
GFRP	12	11.94	-	963.46	52.46	2.98
GFRP	16	15.86	-	938.75	53.24	3.12
Steel	10	10.06	463.24	549.78	200.10	-
Steel	12	12.10	508.66	658.13	197.78	-
Steel	16	16.12	478.54	618.78	204.34	-

2.2 Preparation of Pullout Specimens

The effectiveness of the bond between control concrete supplemented with one-part geopolymer concrete with steel bars and GFRP bars was assessed in accordance with the IS: 2770 (Part I)-2007 code. A total of sixteen sample cubes with steel and GFRP bars measuring 150 mm were manufactured. The testing parameters included the type of concrete, the type of reinforcement, and the diameter of the bar. The GFRP bars' poorer transverse strength causes them to rupture under tensile force at the holding position. In order to capture an effective bond response throughout the pullout test, a steel tube is installed on the supporting end. In order to keep the bar's intended embedding length, a PVC tube is also placed on the other side. The pullout specimens and prepared GFRP bars that were cast in accordance with IS: 2770 (Part I)-2007 are displayed in Figure 2. and left to cure naturally.

Fig. 2. GFRP bars and steel bar pullout specimens

2.3 Test Setup

A 100-ton Universal Testing Machine (UTM) using a pullout frame is shown in Figure 3. An upper plate having a hole larger than the diameter of the bar as well as a lower plate connected by a steel rod make up the testing frame. The test samples had been stored in the frames in order that the UTM's lower jaw held the steel rod in place while its upper jaw was employed to draw the bar. The pullout test was performed in compliance with IS: 2770 (Part I)-2007 to ascertain the loaded end slip, and the loading rate was restricted to less than 22000N/min. The earlier investigations used a similar setup[22].

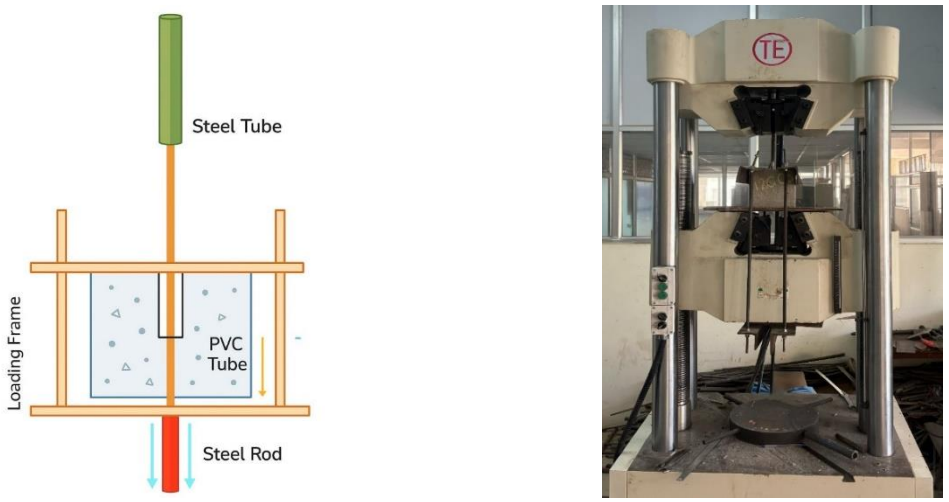

Fig. 3. Pullout test setup: UTM picture and pullout frame schematic diagram

3. Results and Discussions

3.1 Maximum Slide and Pullout Load

The maximum pullout load (P_{max}) as measured by experiment and measurement of slip (S_m) at the loaded end for each of the 16 samples considered are listed in Table 6 of the investigation. Additionally, the average pullout load is displayed and listed in Table 6 of the investigation. Additionally, the mean pullout load is displayed. slip, as well as bond stress values for each of the experimental variables. Figure 5 illustrates how bond specimens exhibit a rise in pullout load as the bar's diameter increases. One-part geopolymer concrete showed a noticeable 14% increase in load when compared to regular concrete. Furthermore, GFRP specimens demonstrated an average 10% decrease in pullout capability in regular concrete when compared to steel bond specimens, but in one-part geopolymer concrete, GFRP bars exhibited almost the same pullout load compared to steel bars[23].

Table 6. Pullout test results

Sl.No.	Specimen	Max Load (kN)	Avg Max Load (kN)	Max Stress (kN/mm²)	Avg max Stress (kN/mm²)	Slip (mm)	Avg Slip (mm)	Failure Mode
1	12CCS-1	48.65	44.42	8.60	7.85	13.67	12.49	S
2	12CCS-2	40.20		7.11		11.30		S
3	12GPS-1	51.15	50.74	9.04	8.96	13.76	13.37	S
4	12GPS-2	50.34		8.89		12.98		S
5	12CCG-1	39.70	39.10	7.02	6.91	9.99	9.69	S
6	12CCG-2	38.50		6.81		9.40		S
7	12GPG-1	50.32	49.65	8.90	8.77	10.20	10.09	S
8	12GPG-2	48.98		8.66		9.98		S
9	16CCS-1	49.35	47.92	6.54	6.35	11.72	11.71	S
10	16CCS-2	46.50		6.16		11.70		S
11	16GPS-1	53.40	52.70	7.08	6.98	15.86	18.21	S
12	16GPS-2	52.00		6.89		20.57		S
13	16CCG-1	44.65	41.95	5.92	5.56	9.24	9.39	S
14	16CCG-2	39.25		5.20		9.54		S
15	16GPG-1	52.40	52.00	6.95	6.89	11.07	10.98	S
16	16GPG-2	51.60		6.84		10.89		S

3.2 Failure Modes of Pullout Specimens

The forms of failure for each tested specimen are also listed in Table 6, with split (S) failure having the most prevalent type. As seen in Figure 4, bond specimens with bars of 12 and 16 mm in diameter have displayed signs of split failure. Shear cracks in the concrete formed

where the bar as well as the surrounding concrete met because the bond-induced separating tensile stress. A similar behavior was encountered in the previous studies[24]. The bond specimens collapsed in a splitting manner because of cracks which were spread to the exterior surface of the concrete. The bars' splitting collapse was caused by split tensile stress being sufficient to disperse shear cracks to the outside of the 12 mm-diameter bars. All of the examples displayed comparable splitting failure when the bar's diameter was increased to 16 mm[25]. The failure characteristics are not significantly affected by the type of concrete. Using one-part concrete instead of regular concrete caused bar scratches and the use of a splitting technique for failure to expose tiny glass fibers enabling bond specimens[26].

Fig. 4. Failure mode of 12 mm steel bars and GFRP bars in concrete

3.3 Bond Stress vs. Slip Curve

The bond-stress vs slip curve was acquired for 16 specimens, as shown in Figure 5. Three regions are commonly observed in curves that exhibit split failure: The ascending area, sometimes referred to as the linear area, is quite rigid and requires the highest force to produce even the smallest amount of slide. The primary causes of the increased stiffness are chemical adhesion on the contact and mechanical interlocking. A modest rise in bond stress in the non-linear region can be regarded as a worsening of the bond response since the slip increases more rapidly due to the decrease in stiffness [27, 28]

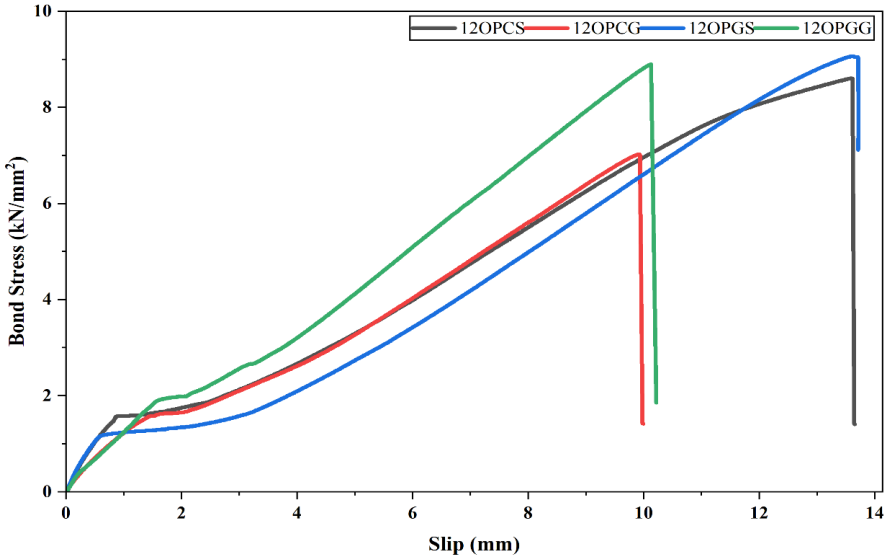

(a)

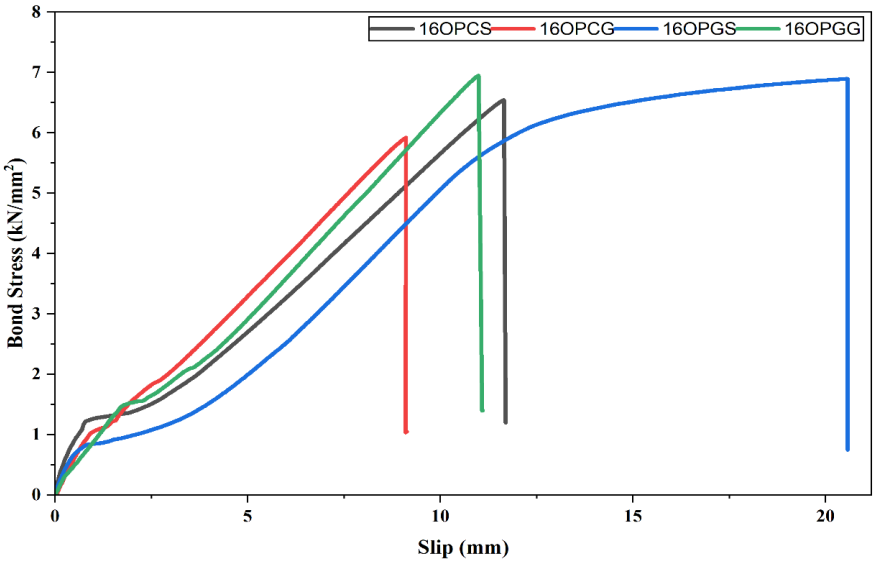

(b)

Fig. 5. Slip curves versus bond stress (a) Concrete made with ordinary Portland cement (OPC) and OPG that contains steel and GFRP bars with a 12 mm diameter (a) Steel and GFRP bars with a diameter of 16 mm in OPC and OPG concrete

Bond stress is also increased by the resistance offered by mechanical interlocking as well as to a lesser degree, the interface frictional force. A decrease in bond stress and an increase in slip value are characteristics of the final softening area. when the pullout load is resisted by the interface frictional force. The linear, nonlinear, as well as softening portions of the bond stress vs slip curves are displayed in Figure 5 for the specimens with 12mm bars. Similar findings were found for samples with bars of 16 mm in diameter. The first slope indicates the chemical adhesion between the bar and the concrete, and the curve shows that the loaded end slides at the beginning of loading [29,30]

3.4 Effect of Type and Diameter of Bar

It is evident from Figure 5 that the bond stress dropped as the bar's diameter increased. A nonlinear normal distribution for stress over the cross-sectional area is the result of differential displacement in GFRP bars with lower axial shear stiffness when they are dragged through the surface[31]. The average normal stress is then connected to the computed bond strength. The shear lag effect is the result of a significant decrease in average normal stress with increasing diameter, which lowers bond strength. Because of this, GFRP bar specimens with lower diameter bars have a higher maximum bond strength than those with larger diameters. As the bar's diameter increases, the pullout load increases because of the specimen's increased cross-sectional area, and the findings are in line with previous research [32-34].

The bond stress vs slip curve for specimens of GFRP and steel bars in regular concrete with one-part geopolymer concrete is shown in Figure 5. The bond specimen cast failed in the splitting mode using the identical diameter, concrete type, and experimental setup and process. The GFRP bond specimens demonstrated a slightly lower adhesion strength of 7.02N/mm^2 with bond strength compared to the steel bond specimen of 8.6N/mm^2 in normal control concrete. In the case of one-part geopolymer concrete, GFRP bars of 12mm diameter showed almost similar bond strength of 8.9/mm^2 in comparison with a steel bar of 9.04N/mm^2. Poor axial shear strength in spite of its smooth surface. However, because to their low elastic modulus, GFRP specimens initially show poor stiffness. Figure 4 shows that the crushing of the concrete is what leads to the failure for steel bar specimens, but the failure of GFRP bars is caused by the surface layer peeling.

3.5 Comparison Between Normal Concrete and One-Part Geopolymer Concrete

One-part geopolymer concrete has a stronger bond than regular control concrete, as seen in Figure 5, because of the lateral confinement effect. The findings are consistent with the research [32]. But with one-part geopolymer concrete, it was shown that a change in the bar's diameter accelerated the rate at which the bond strength decreased. Additionally, the type of concrete has a direct impact on the failure mechanism. In the pullout mode of failure, the bar serves as the failure interface. After that, the strength of the concrete has no bearing on the bond strength. However, in a split mode of failure, the failure interface is located in the concrete matrix; consequently, the strength of the concrete determines the bond strength[33].

4. Conclusions

This study looked at the binding behavior of GFRP bars in both regular concrete as well as one-part geopolymer concrete. Parameters including the diameter for the bars, the form of bars (GFRP and steel) and the concrete type (OPC and OPGC) were investigated. For each sample, the concrete average compressive strength was determined, and for reinforcement in concrete, the average bond strength, slip, failure mode, and bond stress vs. slip relationship were ascertained. The current study yielded the following conclusions:

- Because of the lateral confinement effect, one-part geopolymer concrete has a stronger bond than regular control concrete.
- A change in the bar's diameter accelerated the rate at which the bond strength decreased. Additionally, the type of concrete has a direct impact on the failure mechanism.
- The pullout load rises by up to 8% as the bar's diameter increases. There was also a noticeable increment in the load, 13% in the one-part geopolymer concrete from 44kN to 50.74kN in 12mm diameter bars compared to the control concrete.
- According to the test results, the primary reason why bond specimens failed was concrete splitting. The external surface of the GFRP bar exhibits layer-by-layer shearing and rip peeling as a result of failure. Unbroken ribs as well as shear cracks throughout the concrete on the two 12mm as well as 16mm bars are characteristics of split failure.
- Concrete split failure occurs in both 12mm and 16mm diameter specimens, demonstrating concrete split failure. In this case, the shear strength of the concrete determines the bond strength of the specimen.
- Due of their lower axial modulus, GFRP bar specimens were shown to have a larger loaded slip when compared to steel specimens. Because of the flat surface as well as lower axial shear strength, the specimens also showed decreased stiffness and bond strength. Despite differences in surface condition, GFRP bars are remarkably similar to steel bond specimens.

References

[1] Mahendra K, Narasimhan MC. One part alkali-activated materials for construction - A review. Mater Today Proc. 2023;182-188. https://doi.org/10.1016/j.matpr.2023.07.116

[2] Abdul-Wahab SA, Al-Rawas GA, Ali S, Al-Dhamri H. Assessment of greenhouse CO2 emissions associated with the cement manufacturing process. Environ Forensics. 2016;17(4):338-354. https://doi.org/10.1080/15275922.2016.1177752

[3] Zhao Q, Ma C, Huang B, Lu X. Development of alkali activated cementitious material from sewage sludge ash: Two-part and one-part geopolymer. J Clean Prod. 2023;384:135547. https://doi.org/10.1016/j.jclepro.2022.135547

[4] Toutanji H, Delatte N, Aggoun S, Duval R, Danson A. Effect of supplementary cementitious materials on the compressive strength and durability of short-term cured concrete. Cem Concr Res. 2004;34(2):311-319. https://doi.org/10.1016/j.cemconres.2003.08.017

[5] Revathi T, Vanitha N, Jeyalakshmi R, Sundararaj B, Jegan M, Rajkumar PRK. Adoption of alkali-activated cement-based binders (geopolymers) from industrial by-products for sustainable construction of utility

buildings-A field demonstration. J Build Eng. 2022;52:104450. https://doi.org/10.1016/j.jobe.2022.104450
[6] Osio-Norgaard J, Gevaudan JP, Srubar WV. A review of chloride transport in alkali-activated cement paste, mortar, and concrete. Constr Build Mater. 2018. https://doi.org/10.1016/j.conbuildmat.2018.07.119
[7] Patel YJ, Shah N. Enhancement of the properties of Ground Granulated Blast Furnace Slag based Self Compacting Geopolymer Concrete by incorporating Rice Husk Ash. Constr Build Mater. 2018;171:654-662. https://doi.org/10.1016/j.conbuildmat.2018.03.166
[8] Gholampour A, Ozbakkaloglu T, Ng CT. Ambient- and oven-cured geopolymer concretes under active confinement. Constr Build Mater. 2019;228:116722. https://doi.org/10.1016/j.conbuildmat.2019.116722
[9] Ibrahim M, Maslehuddin M. An overview of factors influencing the properties of alkali-activated binders. J Clean Prod. 2021;124972. https://doi.org/10.1016/j.jclepro.2020.124972
[10] Zhou S, Ma C, Long G, Xie Y. A novel non-Portland cementitious material: Mechanical properties, durability and characterization. Constr Build Mater. 2020;238:117671. https://doi.org/10.1016/j.conbuildmat.2019.117671
[11] Samimi K, Kamali-Bernard S, Maghsoudi AA, Maghsoudi M, Siad H. Influence of pumice and zeolite on compressive strength, transport properties and resistance to chloride penetration of high strength self-compacting concretes. Constr Build Mater. 2017;151:292-311. https://doi.org/10.1016/j.conbuildmat.2017.06.071
[12] Niyazuddin, B U. Experimental investigation on bond behaviour of the GFRP bars with normal and high strength geopolymer concrete. Constr Build Mater. 2024;429:136395. https://doi.org/10.1016/j.conbuildmat.2024.136395
[13] Sofi M, Van Deventer JSJ, Mendis PA, Lukey GC. Bond performance of reinforcing bars in inorganic polymer concrete (IPC). J Mater Sci. 2007;42(9):3107-3116. https://doi.org/10.1007/s10853-006-0534-5
[14] Castel A, Foster SJ. Bond strength between blended slag and Class F fly ash geopolymer concrete with steel reinforcement. Cem Concr Res. 2015;72:48-53. https://doi.org/10.1016/j.cemconres.2015.02.016
[15] Sarker PK. Bond strength of reinforcing steel embedded in fly ash-based geopolymer concrete. Mater Struct. 2011;44(5):1021-1030. https://doi.org/10.1617/s11527-010-9683-8
[16] Parvizi M, Noël M, Vasquez J, Rios A, González M. Assessing the bond strength of Glass Fiber Reinforced Polymer (GFRP) bars in Portland Cement Concrete fabricated with seawater through pullout tests. Constr Build Mater. 2020;263:120952. https://doi.org/10.1016/j.conbuildmat.2020.120952
[17] Zeng JJ, et al. Bond behavior between GFRP bars and seawater sea-sand fiber-reinforced ultra-high strength concrete. Eng Struct. 2022;254:113787. https://doi.org/10.1016/j.engstruct.2021.113787
[18] Kazemi H, Yekrangnia M, Shakiba M, Bazli M, Oskouei AV. Bond-slip behaviour between GFRP/steel bars and seawater concrete after exposure to environmental conditions. Eng Struct. 2022;268:114796. https://doi.org/10.1016/j.engstruct.2022.114796
[19] Lee JY, et al. Interfacial bond strength of glass fiber reinforced polymer bars in high-strength concrete. Compos B Eng. 2008;39(2):258-270. https://doi.org/10.1016/j.compositesb.2007.03.008
[20] Baena M, Torres L, Turon A, Barris C. Experimental study of bond behaviour between concrete and FRP bars using a pull-out test. Compos B Eng. 2009;40(8):784-797. https://doi.org/10.1016/j.compositesb.2009.07.003
[21] Gao K, Li Z, Zhang J, Tu J, Li X. Experimental research on bond behavior between GFRP bars and stirrups-confined concrete. Appl Sci. 2019;9(7):1340. https://doi.org/10.3390/app9071340
[22] Vilanova I, Baena M, Torres L, Barris C. Experimental study of bond-slip of GFRP bars in concrete under sustained loads. Compos B Eng. 2015;74:42-52. https://doi.org/10.1016/j.compositesb.2015.01.006
[23] Kim B, Doh JH, Yi CK, Lee JY. Effects of structural fibers on bonding mechanism changes in interface between GFRP bar and concrete. Compos B Eng. 2013;45(1):768-779. https://doi.org/10.1016/j.compositesb.2012.09.039
[24] Li J, Gravina RJ, Smith ST, Visintin P. Bond strength and bond stress-slip analysis of FRP bar to concrete incorporating environmental durability. Constr Build Mater. 2020;261:119860. https://doi.org/10.1016/j.conbuildmat.2020.119860
[25] Muñoz MB. Study of bond behaviour between FRP reinforcement and concrete [Internet]: http://hdl.handle.net/10803/7771
[26] Godat A, Aldaweela H, Aljaberi H, Al Tamimi N, Alghafri E. Bond strength of FRP bars in recycled-aggregate concrete. Constr Build Mater. 2021;267:120919. https://doi.org/10.1016/j.conbuildmat.2020.120919
[27] Romanazzi V, Leone M, Aiello MA, Pecce MR. Bond behavior of geopolymer concrete with steel and GFRP bars. Compos Struct. 2022;300:116150. https://doi.org/10.1016/j.compstruct.2022.116150

[28] Baena M, Torres L, Turon A, Llorens M, Barris C. Bond behaviour between recycled aggregate concrete and glass fibre reinforced polymer bars. Constr Build Mater. 2016;106:449-460. https://doi.org/10.1016/j.conbuildmat.2015.12.145
[29] Golafshani EM, Rahai A, Sebt MH. Bond behavior of steel and GFRP bars in self-compacting concrete. Constr Build Mater. 2014;61:230-240. https://doi.org/10.1016/j.conbuildmat.2014.02.021
[30] Rolland A, Quiertant A, Khadour A, Chataigner S, Benzarti K, Argoul P. Experimental investigations on the bond behavior between concrete and FRP reinforcing bars. Constr Build Mater. 2018;173:136-148. https://doi.org/10.1016/j.conbuildmat.2018.03.169
[31] Tighiouart B, Benmokrane B, Gao D. Investigation of bond in concrete member with fibre reinforced polymer FRP bars. 1998. https://doi.org/10.1016/S0950-0618(98)00027-0
[32] Gu X, Yu B, Wu M. Experimental study of the bond performance and mechanical response of GFRP reinforced concrete. Constr Build Mater. 2016;114:407-415. https://doi.org/10.1016/j.conbuildmat.2016.03.211
[33] Saleh N, Ashour A, Lam D, Sheehan T. Experimental investigation of bond behaviour of two common GFRP bar types in high - Strength concrete. Constr Build Mater. 2019;201:610-622. https://doi.org/10.1016/j.conbuildmat.2018.12.175
[34] Dahou Z, Castel A, Noushini A. Prediction of the steel-concrete bond strength from the compressive strength of Portland cement and geopolymer concretes. Constr Build Mater. 2016;119:329-342. https://doi.org/10.1016/j.conbuildmat.2016.05.002